Lorentz TEM investigation of chiral spin textures and Néel Skyrmions in asymmetric [Pt/(Co/Ni)_{M}/Ir]_{N} multi-layer thin films

Maxwell Li, Derek Lau, Marc De Graef, and Vincent Sokalski

Lorentz TEM investigation of chiral spin textures and Néel Skyrmions in asymmetric [Pt/(Co/Ni)$_M$/Ir]$_N$ multi-layer thin films

Maxwell Li,* Derek Lau, Marc De Graef, and Vincent Sokalski

Department of Materials Science & Engineering,
Carnegie Mellon University, Pittsburgh, Pennsylvania 15213, USA

(Dated: May 25, 2019)

We examine magnetic domain patterns in symmetric [Co/Ni]$_M$ and asymmetric [Pt/(Co/Ni)$_M$/Ir]$_N$ multi-layers using Fresnel mode Lorentz transmission electron microscopy (LTEM). In the symmetric multi-layers, where the Dzyaloshinskii-Moriya Interaction is expected to be negligible, we observe Bloch type domain walls with no preferred chirality. In the asymmetric multi-layers, where significant interfacial DMI is present, we observe domain patterns with chiral Néel domain walls, which evolve into sub-100nm isolated Néel Skyrmions with the application of a perpendicular field at room temperature. The impact of layer thickness and film stack on interfacial magnetic properties is discussed in the context of developing a tunable multi-layer system for future spintronic applications.

I. INTRODUCTION

Chiral domain walls (DWs) and magnetic objects with added topological stability, such as Skyrmions, have garnered a great deal of attention in recent years due the unprecedented efficiency by which they can be manipulated with electric current for use in future spintronic devices [1–3]. Skyrmions are described by the topological charge, C, as determined from $4\pi C = \int \mathbf{m} \cdot (\partial_x \mathbf{m} \times \partial_y \mathbf{m}) \, \mathrm{d}x\mathrm{d}y$. They can also be described by a polarity ($p = \pm 1$), which indicates the magnetization direction at the center of the Skyrmion, and helicity (γ) that gives the direction of internal magnetization along the circumference [4]. Such objects are stabilized by the Dzyaloshinskii-Moriya interaction (DMI) which is found in magnetic materials where inversion symmetry is broken [5, 6]. This interaction has been observed in bulk magnetic materials lacking inversion symmetry (such as FeGe [7] and MnSi [8]) and more recently in magnetic multi-layers at the interface of a ferromagnet (FM) and a heavy metal (HM) with large spin-orbit coupling [9–11]. In the latter case, interfacial DMI is well-established to stabilize chiral Néel walls over the magnetostatically favorable Bloch wall [12].

The discovery of DMI has opened the door to a range of new magnetic materials and multi-layer designs to support the formation of such chiral configurations. Parameters such as FM/HM interfaces [13–15], FM layer composition [16], and asymmetric stacking sequences [17] have been explored as means of strengthening DMI in multi-layer systems. The ideal system will offer tunability of emergent magnetic properties, including DMI, while preserving other critical properties such as magnetic anisotropy and saturation magnetization.

In this work we examine the magnetic domain structures of asymmetric multi-layers based on [Pt/(Co/Ni)$_M$/Ir]$_N$ using Lorentz transmission electron microscopy (LTEM). Interfacial DMI is induced at the HM/FM interface. It has been reported that Pt and Ir induce DMI of opposite sign leading to an additive effect when placed on opposite surfaces of a magnetic heterostructure [13, 18]. Although some reports have found both the Pt/Co and Ir/Co interfaces produce DMI of the same sign [3, 19], it is still agreed that the magnitude of DMI at the Pt/Co interface is much larger. As shown in the supplementary information of this manuscript, we have leveraged the asymmetric bubble expansion technique [10, 20, 21] to determine interfacial DMI for $M = 2$ and $N = 1$ [22]. In films used for the Lorentz TEM investigation, the number of Co/Ni layers, M, offers tunability of interfacial magnetic properties, such as DMI, while the number of total repeats, N, contributes to the stabilization of stripe domain patterns [23, 24]. These characteristics are reflected in Fresnel mode LTEM images to follow. We note that the inclusion of Ni in the multi-layer allows us to increase the magnetic layer thickness (via M), thereby reducing DMI, but preserves perpendicular magnetic anisotropy due to the Co/Ni interface. This would not be possible in a multi-layer based only on Pt/Co/Ir. Symmetric [Co/Ni]$_M$ based multi-layers, which are expected to have negligible DMI, were also examined with LTEM for comparison.

II. EXPERIMENTAL

Multi-layers were deposited onto 10 nm thick amorphous Si$_3$N$_4$ membranes via magnetron sputtering in an Ar environment with working pressure fixed at 2.5 mTorr and base pressure at $< 3.0 \times 10^{-7}$ Torr. All film stacks were deposited onto seedlayers of Ta(3 nm)/Pt(3 nm) with capping layers of Pt(3 nm)/Ta(3 nm). Asymmetric and symmetric multi-layers had the following subsequent layers: [Pt(0.5 nm)/(Co(0.2 nm)/Ni(0.6 nm))$_M$/Ir(0.5

* mpli@andrew.cmu.edu

nm)]$_N$ and [Co(0.2 nm)/Ni(0.6 nm)]$_M$/Co(0.2), respectively. Magnetic hysteresis loops of these multi-layers were measured using alternating gradient field magnetometry (AGFM) and vibrating sample magnetometry (VSM) to determine M_S and K_{eff}. K_{eff} was determined from the area between in-plane and perpendicular loops.

Fresnel mode LTEM imaging was performed on an aberration-corrected FEI Titan G2 80-300 operated in Lorentz mode at room temperature. Magnetic induction maps were produced by solving the Transport of Intensity Equation (TIE) using over- and under-focused Fresnel images as in [25]. In some cases, a perpendicular magnetic field was applied in-situ by exciting the objective lens of the microscope. Interfacial DMI affects domain wall characteristics most notably manifesting in the formation of Néel walls over the magnetostatically favorable Bloch wall [12]. In the absence of specimen tilt, Néel walls do not display magnetic contrast as the deflection of electrons through the Lorentz force lies parallel to the DW. When a sample tilt is applied, however, the perpendicular magnetic induction of surrounding domains gains an effective in-plane induction which deflects electrons towards or away from the DW, leading to the appearance of magnetic contrast [26, 27]. This is not the case for Bloch walls which form magnetic contrast in the absence of sample tilt as electrons are deflected perpendicular to the DW.

III. SYMMETRIC CO/NI MULTI-LAYERS

Symmetric [Co/Ni]$_M$ based multi-layers were first examined to serve as a limiting case where there is no impact from Ir and Pt. The shearing and pinched shape of the perpendicular M-H loop, which is characteristic of bubble materials, suggests the formation of a multi-domain state at zero applied field [23, 24]. The increased loop shearing at $M = 100$, compared to $M = 10$, is due to the increased role of dipole-dipole interactions in the formation of small magnetic domains when films are thicker. We note a negative nucleation field of 400 mT for $M = 100$ as compared to 5 mT for $M = 10$.

Fresnel mode LTEM images of both symmetric multi-layers ($M = 10, 100$) display magnetic contrast in the absence of tilt (FIG. 1c & d)due to the Bloch component of the internal DW magnetization, which does not have any preferred chirality in this system. It is possible that the DW adopts a hybrid "twisted" DW structure due to dipolar interactions where the wall transitions through a Bloch point between anti-parallel Néel caps [28–30]. This is especially likely in the $N = 100$ sample where a gradual transition through the thickness reduces exchange energy of the hybrid wall. However, because the electron beam is insensitive to any Néel component of the DW in the untilted orientation, we are not able to confirm this experimentally.

The domain structure of the sample with $M = 100$

displays a demagnetized labyrinth-configuration with periodic domain spacing, typical of bubble materials, as anticipated from the M-H loops. The domain structure for $M = 10$ is more stochastic with much larger domains that do not arrange in any periodic fashion. This behavior is expected as the dipolar energy that stabilizes the labyrinth pattern in thicker samples becomes less significant. Vertical Bloch lines (VBLs) are also observed in these multi-layers which are decribed by 180° rotations in magnetic induction along a DW [31]. This appears as a discontinuity in contrast along a DW in Fresnel mode images whereby the contrast inverts about the discontinuity.[32] Such VBLs are observed to occur at a high frequency in the $M = 10$ multi-layers forming clusters whereby several VBLs exist at close proximity with one another along a DW [33]. VBLs are also observed in $M = 100$ multi-layers but are more sporadic and not found to form clusters as in the $M = 10$ sample. Application of an ex-situ in-plane magnetic field produces a stripe domain pattern with domains aligned parallel to the field direction as shown in FIG. 2a & b. An in-situ perpendicular magnetic field leads to the formation of magnetic bubbles, which are found to be Bloch type ($C = 1$) having no preferred chirality ($\gamma = \pm\pi/2$) or topo-
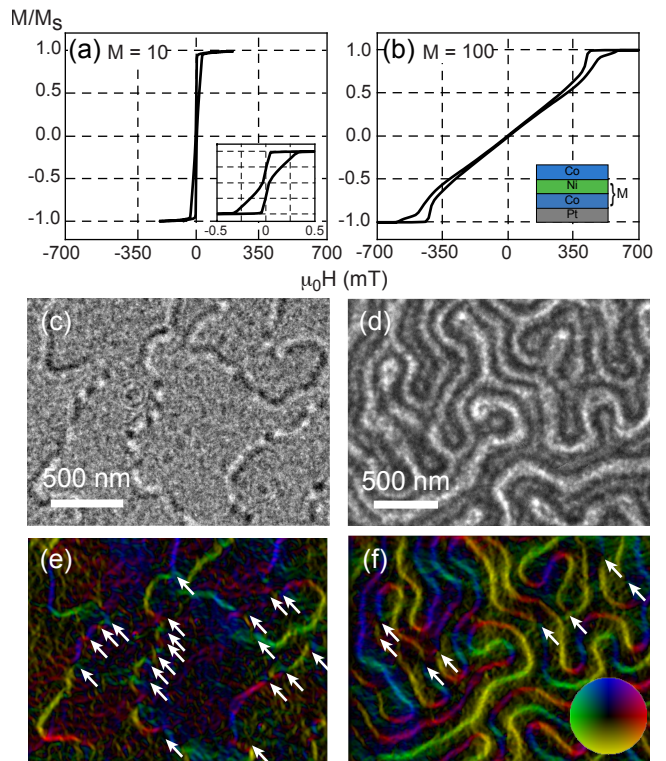

FIG. 1. Perpendicular M-H loops, Fresnel mode image, and calculated in-plane induction maps of symmetric [Co/Ni]$_M$ multi-layers where $M = 10$ (a,c,e) and 100 (b,d,e). Arrows designate locations of vertical Bloch lines in in-plane induction maps. Inset depicts $M = 10$ loop with a smaller field of view and schematic of symmetric film stack.

logically trivial ($C = 0$) where two VBLs are present along the circumference (see example in supplementary information) [22, 34].

IV. ASYMMETRIC PT/CO/NI/IR MULTI-LAYERS

The tunability of asymmetric $[Pt/(Co/Ni)_M/Ir]_N$ based multi-layers was examined by varying the number of Co/Ni layers in a repeat unit, M. The total number of repeat units in a multi-layer stack, N, was used to stabilize labyrinth domain patterns. By increasing M, the effective DMI is expected to decrease while the areal magnetization will increase. We note that the interfacial anisotropy associated with Co/Ni is comparable to that of Co/(Pt, Ir) so we do not expect a loss of perpendicular magnetic anisotropy (PMA). We also note that increasing thickness of either Co or Ni would lead to a decrease in PMA, which could be useful for stabilization of Skyrmions in subsequent studies. Broadly, this tunability would allow for the exploration of a wider parameter space in the design of chiral magnetic systems.

M-H loops of asymmetric multi-layers (FIG. 3) indicate PMA is preserved with the addition of heavy metal layers in the repeat structure. As with the symmetric case, the loop becomes more sheared with increasing M and has a similar pinched hysteresis. M_s and K_{eff} both increase monotonically with increasing Co/Ni repeats ($M = 1, 2, 3$) for the case of $N = 5$ or 10. These trends are included in the supplemental material provided with this manuscript [22].

Fresnel mode LTEM images of these asymmetric multi-layers only display magnetic contrast upon tilting (FIG. 4). The lack of magnetic contrast in the untilted state sugg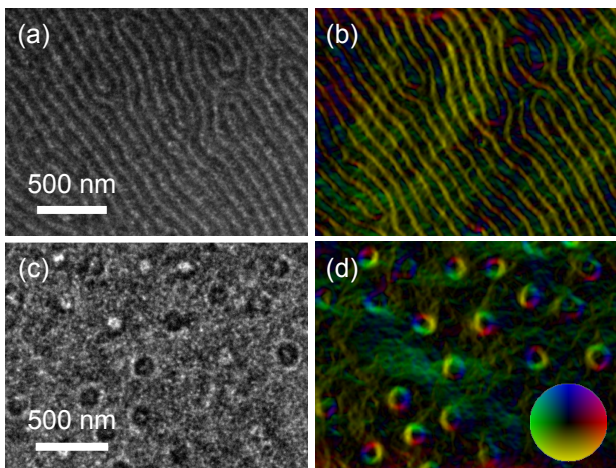ests that there is no Bloch component to these do-main walls (i.e. fully Néel). The contrast seen in the accompanied in-plane induction map of FIG. 4c calculated from the tilted Fresnel images is due to the magnetization of the domains, which now have a component perpendicular to the electron beam. This process reveals alternating perpendicular domains, but does not directly provide any details on the internal structure of the domain walls.

As such we proceed on characterizing the domain patterns in asymmetric films by direct examination of the Fresnel images. For N = 5, magnetic contrast characteristic of Néel walls is observed even when M is increased from 1 to 3 despite a purported reduction in DMI. We note that a relatively large DMI ($D = -0.39$ mJ/m^2) was measured for $M = 2$, $N = 1$ so it is not surprising that a 50% increase in thickness is insufficient to reduce D below the critical value required to overcome the DW anisotropy [22]. A labyrinth domain structure is observed in each of these multi-layers with DW contrast becoming more apparent as M increases due to greater magnetic induction originating from a larger ferromagnetic thickness. Despite changes to DMI and perpendicular magnetic anisotropy, the domain widths are not observed to change greatly between $M = 2$ and 3.

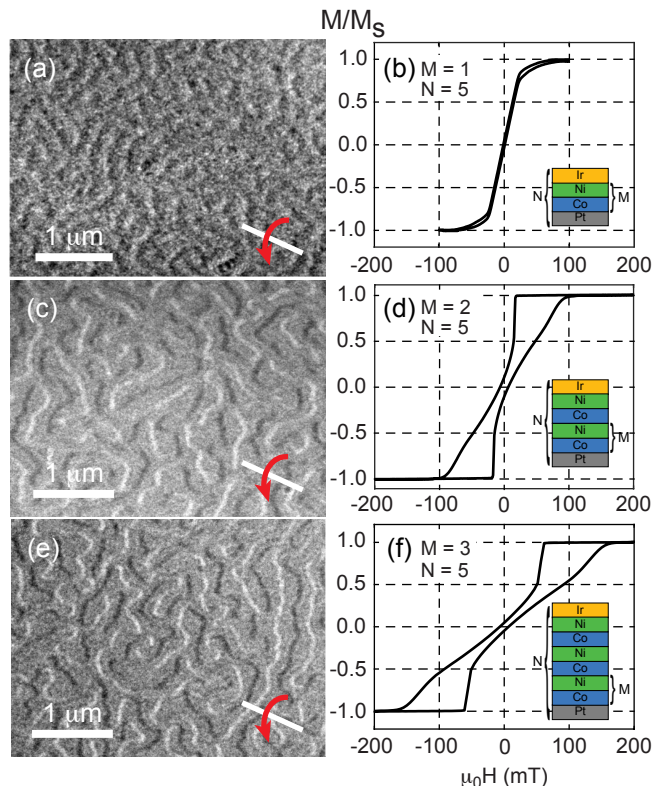Next we examined the effects the number of film stack

FIG. 3. Fresnel mode Lorentz TEM images and perpendicular M-H loops of asymmetric asymmetric $[Pt/(Co/Ni)_M/Ir]_{10}$ multi-layers where $M =$ (a,b) 1, (c,d) 2, or (e,f) 3. Sample tilt of 20° is present in each image. Insets depict schematic of asymmetric film stack.
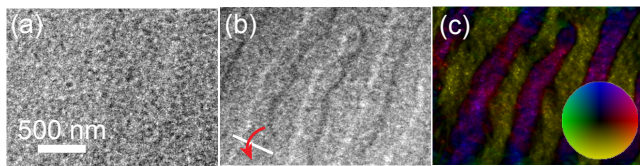

FIG. 2. Fresnel mode LTEM images (a,c) and respective in-plane induction maps (b,d) of symmetric $[Co/Ni]_{100}$ multilayers (a,b) after ex-situ in-plane saturation and (c,d) with static in-situ perpendicular field, $H_z = 480$ mT.

FIG. 4. Fresnel mode Lorentz TEM images of $[Pt/(Co/Ni)_2/Ir]_5$ (a) for no tilt and (b) $20°$ tilt. (c) In-plane induction map calculated from tilted through-focus images.
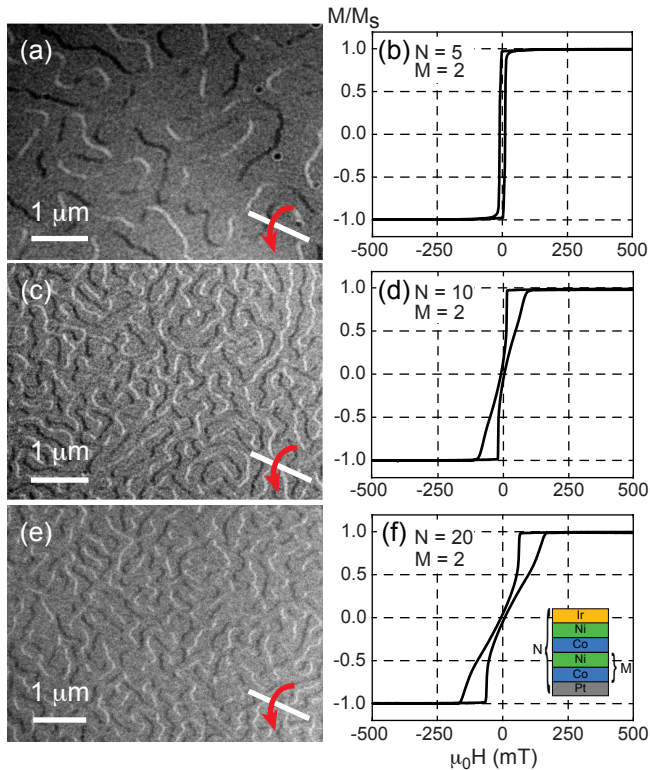

FIG. 5. Fresnel mode Lorentz TEM images and perpendicular M-H loops of asymmetric $[Pt/(Co/Ni)_2/Ir]_N$ where N = (a,b) 5, (c,d) 10, and (e,f) 20. Samples were tilted by $20°$ for each image. Inset depicts schematic of asymmetric film stack.

repeats, N, has on magnetic domain characteristics in $[Pt/(Co/Ni)_2/Ir]_N$ where N = 5, 10 or 20 (FIG. 5). Again, magnetic contrast was only observed in the presence of sample tilt in these films suggesting that there is no appreciable Bloch component [22]. Magnetic domains when $N = 5$ were noticeably wider than those for $N = 10$ and 20 which is also observed with symmetric films. A perpendicular magnetic field was applied in-situ on $[Pt/(Co/Ni)_2/Ir]_{20}$ multi-layers by exciting the objective lens of the TEM (FIG. 6). With increasing field, domains with magnetization anti-parallel to the direction of the field shrink and visa versa. Near the saturation field, these domains form isolated Néel Skyrmions with diameters of $\sim$80 nm (FIG. 6c) before annihilating. The inversion of contrast upon reversal of focus confirms the magnetic origin of these features (see supplementary

info). The polarity of the observed Skyrmions here is $p = +1$, but the helicity cannot be determined based on the Fresnel mode images alone. In light of the previously determined chirality of this system from Kerr microscopy, we assume the helicity, $\gamma = 0$ (i.e. left-handed Néel walls). Skyrmions were not observed to form in $[Pt/(Co/Ni)_2/Ir]_N$ multi-layers where $N = 5$ or 10 and instead formed long, worm-like domains before annihilating at the saturation field (see supplementary info [22]).

Finally, for the thicker samples, we discuss the possibility that dipolar interactions could stabilize a hybrid DW structure even with an appreciable DMI as observed recently in Co based multi-layers [29, 30]. Taking the limiting case of $M = 3$, $N = 10$ as an example (see supplemental, $M_S = 800$ kA/m and purported $D \sim$ -0.2 mJ/m^3), one would expect a hybrid DW structure based on micromagnetic energy minimization [29, 30]. The absence of any experimentally observable Bloch component here could be due to an underestimation of DMI or overestimation of M_S. We note that the DMI values are based on domain expansion for single layers and may not reflect the properties of these superlattices. We also note that M_S as determined in this work was based only on the thickness of the magnetic material (i.e. Co/Ni). The effective magnetic thickness of the Pt and Ir due to proximity induced magnetization would yield a smaller overall M_S, which would reduce the stability of a hybrid DW structure. It is also possible that the Bloch signal from the hybrid wall was simply not resolvable. Having clearly observed a Bloch component in symmetric films with thicknesses ranging from 5-80 nm, we do not think this is the case.
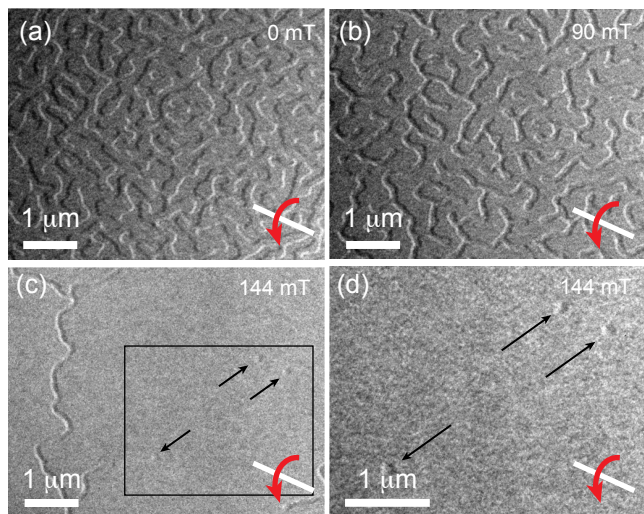

FIG. 6. Fresnel mode Lorentz TEM images of asymmetric $[Pt/(Co/Ni)_2/Ir]_{20}$ with increasing perpendicular magnetic field applied in-situ. Arrows indicate positions of Néel Skyrmions in (c) and (d). Samples were tilted by $20°$ for each image.

V. SUMMARY

In summary, we have examined asymmetric Pt/Co/Ni/Ir based multi-layers using Lorentz transmission electron microscopy. The properties of these multi-layers were tuned through variations in ferromagnetic layer thickness and overall thickness, which were reflected in the magnetic domain structure. Symmetric Co/Ni multi-layers displayed a prominent Bloch component suggesting a weak DMI; with the addition of a Pt and Ir layer sandwiching Co and Ni, DMI is induced which is reflected in the absence of a measurable Bloch component to the walls in Fresnel mode images. Although the effective DMI is expected to diminish with greater ferromagnetic content in film stack repeats, a Bloch component was not observed up to 3 repetitions of the Co/Ni layer. Additionally, asymmetric Pt/Co/Ni/Ir multi-layers with greater number of total film stack repeats were observed to support the formation of sub-100 nm Skyrmions at room temperature in the presence of a perpendicular magnetic field. Overall, this materials system provides a tunable platform for further exploration of chiral spin textures and the development of spintronic devices.

ACKNOWLEDGEMENTS

[1] D. Bromberg, M. Moneck, V. Sokalski, J. Zhu, L. Pileggi, and J.-G. Zhu, in *2014 IEEE International Electron Devices Meeting* (IEEE, 2014) pp. 33–1.

[2] S. Emori, U. Bauer, S.-M. Ahn, E. Martinez, and G. S. D. Beach, Nat. Mater. **12**, 611 (2013).

[3] K.-S. Ryu, S.-H. Yang, L. Thomas, and S. S. P. Parkin, Nat. Commun. **5**, 3910 (2014).

[4] N. Nagaosa and Y. Tokura, Nat. Nanotechnol. **8**, 899 (2013).

[5] I. Dzyaloshinsky, J. Phys. Chem. Solids **4**, 241 (1958).

[6] T. Moriya, Phys. Rev. **120**, 91 (1960).

[7] X. Z. Yu, N. Kanazawa, Y. Onose, K. Kimoto, W. Z. Zhang, S. Ishiwata, Y. Matsui, and Y. Tokura, Nat. Mater. **12**, 106 (2011).

[8] X. Z. Yu, A. Kikkawa, D. Morikawa, K. Shibata, Y. Tokunaga, Y. Taguchi, and Y. Tokura, Phys. Rev. B **91**, 054411 (2015).

[9] A. Thiaville, S. Rohart, E. Jue, V. Cros, and A. Fert, Europhys. Lett. **100**, 57002 (2012).

[10] A. Hrabec, N. A. Porter, A. Wells, M. J. Benitez, G. Burnell, S. McVitie, D. McGrouther, T. A. Moore, and C. H. Marrows, Physical Review B **90**, 020402(R) (2014).

[11] J. P. Pellegren, D. Lau, and V. Sokalski, Phys. Rev. Lett. **119**, 027203 (2017).

[12] A. Thiaville, Journal of Magnetism and Magnetic Materials **140-144**, 1877 (1995).

[13] G. Chen, T.-P. Ma, A. T. N'Diaye, H.-Y. Kwon, C.-Y. Won, Y.-Z. Wu, and A. K. Schmid, Nat. Commun. **4**, 2671 (2013).

[14] H.-X. Yang, O. Boulle, V. Cros, A. Fert, and M. Chshiev, Sci. Rep. **8**, 12356 (2018).

[15] D. Khadka, S. Karayev, and S. X. Huang, J. Appl. Phys. **123**, 123905 (2018).

[16] A. Soumyanarayanan, M. Raju, A. L. G. Oyarce, A. K. C. Tan, M.-Y. Im, A. P. Petrović, P. Ho, K. H. Khoo, M. Tran, C. K. Gan, F. Ernult, and C. Panagopoulos, Nat. Mater. **16**, 898 (2017).

[17] J. H. Franken, M. Herps, H. J. M. Swagten, and B. Koopmans, Sci. Rep. **4**, 5248 (2014).

[18] C. Moreau-Luchaire, C. Moutafis, N. Reyren, J. Sampaio, C. A. F. Vaz, N. V. Horne, K. Bouzehouane, K. Garcia, C. Deranlot, P. Warnicke, P. Wohlhuter, J.-M. George, M. Weigand, J. Raabe, V. Cros, and A. Fert, Nat. Nanotechnol. **11**, 444 (2016).

[19] D. Lau, J. P. Pellegren, H. T. Nembach, J. M. Shaw, and V. Sokalski, Phys. Rev. B **98**, 184410 (2018).

[20] S.-G. Je, D.-H. Kim, S.-C. Yoo, B.-C. Min, K.-J. Lee, and S.-B. Choe, Phys. Rev. B **88**, 214401 (2013).

[21] R. Lavrijsen, D. M. F. Hartmann, A. van den Brink, Y. Yin, B. Barcones, R. A. Duine, M. A. Verheijen, H. J. M. Swagten, and B. Koopmans, Phys. Rev. B **91**, 104414 (2015).

[22] See Supplemental Material at [URL will be inserted by publisher] for measurement of DMI and additional Lorentz TEM images, which includes [10, 11, 19, 35].

[23] C. Kooy and U. Enz, Philips Res. Rep. **15**, 7 (1960).

[24] J. A. Cape and G. W. Lehman, J. Appl. Phys. **42**, 5732 (1971).

[25] C. Phatak, O. Heinonen, M. De Graef, and A. Petford-Long, Nano Lett. **16**, 4141 (2016).

[26] M. J. Benitez, A. Hrabec, A. P. Mihai, T. A. Moore, G. Burnell, D. McGrouther, C. H. Marrows, and S. McVitie, Nat. Commun. **6**, 8957 (2015).

[27] S. McVitie, S. Hughes, K. Fallon, S. McFadzean, D. McGrouther, M. Krajnak, W. Legrand, D. Maccariello, S. Collin, K. Garcia, N. Reyren, V. Cros, A. Fert, K. Zeissler, and C. H. Marrows, Sci. Rep. **8**, 5703 (2018).

[28] M. Labrune and L. Belliard, Phys. Status Solidi A **174**, 483 (1999).

[29] I. Lemesh and G. S. D. Beach, Phys. Rev. B **98**, 104402 (2018).

[30] W. Legrand, J.-Y. Chauleau, D. Maccariello, N. Reyren, S. Collin, K. Bouzehouane, N. Jaouen, V. Cros, and A. Fert, Sci. Adv. **4**, eaat0415 (2018).

[31] A. Malozemoff and J. Slonczewski, Phys. Rev. Lett. **29**, 952 (1972).

[32] R. Cheng, M. Li, A. Sapkota, A. Rai, A. Pokhrel, T. Mewes, C. Mewes, D. Xiao, M. De Graef, and V. Sokalski, Physical Review B **99**, 184412 (2019).

[33] A. Zvezdin and A. Popkov, Zh. Eksp. Teor. Fiz **91**, 1789 (1986).

[34] N. Nagaosa, X. C. Yu, and Y. Tokura, Phil. Trans. R. Soc. A **370**, 5806 (2012).

[35] D. Lau, V. Sundar, J.-G. Zhu, and V. Sokalski, Phys. Rev. B **94**, 060401(R) (2016).